Research Article

Dingyu Ni, Shengliang Lu*, Feng Cai

Performance repair of building materials using alumina and silica composite nanomaterials with electrodynamic properties

https://doi.org/10.1515/chem-2024-0052 received February 23, 2024; accepted May 26, 2024

Abstract: In recent years, the service life of building materials has become the focus of attention. Among them, the service life of concrete and steel bars is particularly affected by the corrosion of external ions (such as Cl-) in the environment. To solve this problem, a new type of composite nanocolloid was prepared through a controllable preparation method. The composite nanocolloid is prepared from aluminum chloride sol and silica sol as raw materials. The prepared colloidal particles have a particle size distribution between 10.5 and 17.5 nm, exhibiting excellent stability and dispersibility. In order to verify the improvement effect of the composite nanocolloid on the properties of building materials, the influence of it on the porosity of concrete and the anti-corrosion performance of steel bars was experimentally studied. The results indicate that the moisture absorption and dehumidification speed of concrete treated with composite nano colloids is slower, and the pore size distribution is mainly concentrated in 100-1,000 nm, indicating that the colloids can effectively optimize the pore structure of concrete. In addition, the processed steel plate samples showed high AC impedance values and low corrosion current logarithmic values in electrochemical testing, indicating that composite nanocolloids have a significant protective effect on the corrosion of steel bars, which can effectively improve the performance of building materials and extend their service life.

Keywords: concrete, building materials, composite nanocolloids, aluminum chloride sol, silica sol, steel bars, electrokinetic properties, chemistry and chemical engineering

1 Introduction

Concrete and steel bars, as materials widely used in construction and infrastructure projects, bear huge structural load-bearing and protection functions [1,2]. However, due to long-term use and erosion from the external environment, reinforced concrete structures are prone to damage and destruction, which in turn affects the stability and service life of the structure [3–5]. Therefore, it is of great significance to study reinforced concrete repair materials and repair methods. Through experiments and analysis, Aykac and Yavuzcan explored the improvement of the strength and durability of beam structures by the epoxy injection repair method. Research results show that epoxy injection can effectively repair damaged reinforced concrete beams and improve their load-bearing capacity and seismic performance [6]. Bahij et al. used low-cost, corrosionresistant cementing materials to strengthen the structural performance of reinforced concrete beams. They discussed the shear, bending, torsion, deflection, crack propagation, and torsion angle of reinforced beams, and proposed that they are suitable for use under different load conditions. Methods for strengthening reinforced concrete beams [7]. These studies provide some ideas that can be used for reference on the topic of reinforced concrete repair. However, the importance of reinforced concrete and other building materials to people's livelihood is self-evident. If concrete structures can be repaired multiple times and quickly, the performance of reinforced concrete will be greatly improved. This puts forward certain requirements for the materials and methods of repairing reinforced concrete [8-10]. Studies have shown that Al₂O₃-SiO₂ nanocolloid can form a tight bond with the surface of reinforced concrete, provide good adhesion, and avoid delamination and cracking between the repair material and the base material. Moreover, the Al₂O₃–SiO₂ nanocomposite colloid is resistant to chemical erosion and can effectively prevent chemical substances such as acids, alkalis, and salts in the external environment from corroding the reinforced

^{*} Corresponding author: Shengliang Lu, Wenzhou Polytechnic, Wenzhou, 325035, China, e-mail: lsl_wzpt@163.com Dingyu Ni, Feng Cai: Wenzhou Polytechnic, Wenzhou, 325035, China

concrete structure [11]. In addition, Al₂O₃-SiO₂ nanocomposite colloid has smaller particle size and higher specific surface area, which can improve the density and stability of repair materials, thereby extending the service life of repair materials [12]. However, the preparation process of Al₂O₃-SiO₂ nanocomposite colloid is relatively complex and the material cost is high, resulting in high repair costs [13]. And due to the special properties of nanocomposite colloids, the construction process needs to be strictly controlled and the technical requirements are high [14]. To this end, a controllable preparation scheme of Al₂O₃-SiO₂ nanocomposite colloid was studied and designed to explore the conductive properties of its colloidal particles, improve the void ratio of concrete and the corrosion protection properties of steel bars. This research has great practical significance for repairing reinforced concrete structures, and also provides certain reference value for the research of Al₂O₃-SiO₂ nanocomposite colloid.

The content of the article can be mainly divided into three parts. The first part mainly explains the preparation and performance testing methods of Al_2O_3 – SiO_2 nanocomposite colloid; the second part analyzes the properties of Al_2O_3 – SiO_2 nanocomposite colloid based on the performance testing method; the third part is about Al_2O_3 – SiO_2 nanocomposite colloid and the summary of performance and research shortcomings.

The main innovation of this study lies in the use of controllable preparation schemes to prepare a stable Al_2O_3 – SiO_2 nanocomposite colloid that exists in a large temperature range and multi-scale distribution range, for the repair of building materials such as concrete. This new

type of composite nano colloid not only has excellent stability and dispersibility, but also shows good effects in treating concrete and steel bars, which can effectively extend the service life of building materials, improve the stability and safety of building structures.

2 Materials and method

2.1 Controllable preparation scheme of Al₂O₃-SiO₂ nanocomposite colloids

 Al_2O_3 – SiO_2 nanocomposite colloid with electrodynamic properties has good mechanical properties and electrical conductivity, and can effectively repair concrete structures. The composite colloid is mainly prepared from $AlCl_3$ sol and silica sol as raw colloids. Specifically, the preparation process is shown in Figure 1.

As shown in Figure 1, the first step is to prepare aluminum chloride sol: (a) At 20°C, mix 200 g of deionized water (AR, Thermo Fisher pure water system) and 91.6 g of crude polyaluminum chloride powder (IG, Tailong Chemical Technology Co., Ltd) and use a magnetic stirrer to stir thoroughly and evenly, to ensure that the powder is completely dissolved and the mixture is uniform. (b) Distribute the mixed solution into four 50 mL centrifuge tubes. The centrifuge tube needs to have sufficient capacity and sealing. (c) Place the centrifuge tubes one by one into the high-speed centrifuge (model TG24-WS, produced by

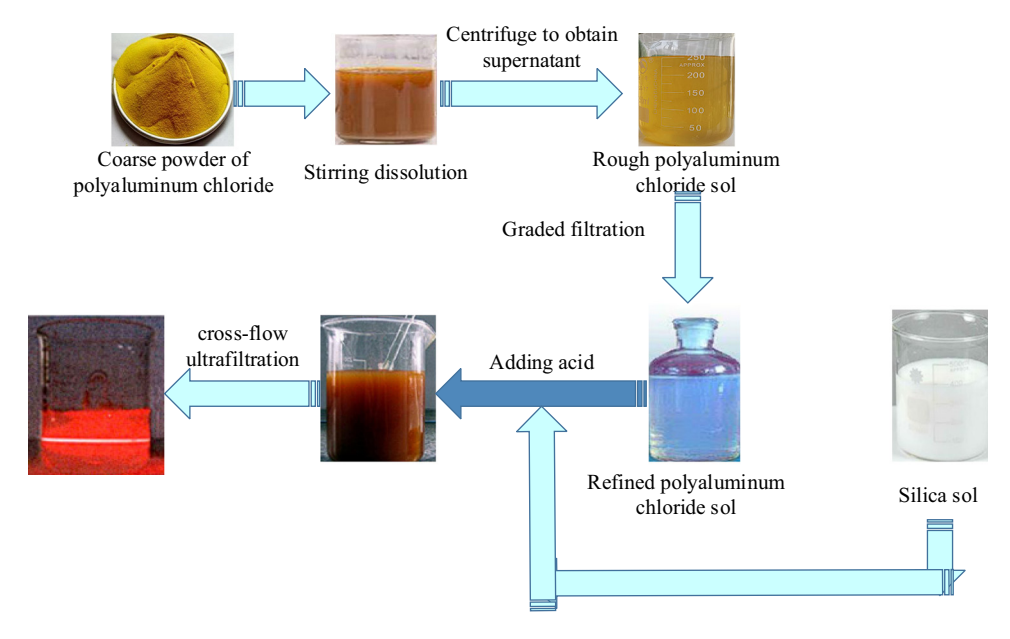


Figure 1: Preparation process of Al₂O₃-SiO₂ nanocomposite colloid.

Sichuan Xiangcheng Centrifuge Co., Ltd), and set the centrifuge speed to 3,000 rpm. After centrifugation for 5 min, it can be observed that the solid particles in the solution are effectively separated and the clear liquid located in the upper layer is extracted. (d) Filter the clear liquid through ultrafiltration membranes with molecular weights of 100,000 and 30,000. This step is to further remove impurities and undissolved particles from the solution, in order to obtain pure polyaluminum chloride nanosols.

The second step is to prepare Al₂O₃-SiO₂ nanosol: (a) Use deionized water to dilute the silica sol (IG, Qingdao Ocean Chemical Co., Ltd) to 10 wt%. (b) Slowly add the previously prepared polyaluminum chloride nanosol to the diluted silica sol, while gently stirring to mix evenly. After dripping, let the mixture stand for 5 min to allow the two sols to fully mix and react. (c) Add 3 mL hydrochloric acid (HCL) (IG, Tailong Chemical Technology Co., Ltd) dropwise to maintain the stability of the sol system. This is to adjust the pH value of the solution and prevent the sol from agglomerating or precipitating in the subsequent process. (d) Pour 500 mL of the prepared sol into a tangential flow ultrafiltration machine and use an ultrafiltration membrane cell with a molecular weight of 30,000 for ultrafiltration to separate particles with a molecular weight less than 30,000. The ultrafiltration machine blocks particles with a molecular weight greater than 30,000 and discharges them through the return port. (e). During the entire process, equal volumes of deionized water are regularly compensated, and ultrafiltration is performed repeatedly to wash away solutes such as H⁺, Cl⁻, Fe³⁺, Na⁺, and K⁺ in the sol until the predetermined preparation requirements are met. (f) During the preparation process, it is necessary to closely monitor the changes in the conductivity and pH value of Al₂O₃–SiO₂ nanocomposite colloids. These two parameters have a significant impact on the stability and performance of colloids. By adjusting the amount of HCL added and the ultrafiltration time, we can control the conductivity between 3.00 and 4.00 S/cm and the pH value between 2 and 4, thereby ensuring that the Al₂O₃-SiO₂ nanocomposite colloid has superior performance.

The applied characteristics are (1) Sol gel characteristic reaction: when the polyaluminum chloride nano sol is mixed with the diluted silica sol, the ions or molecules in the two sols will undergo hydrolysis and condensation reaction, forming new chemical bonds and generating Al₂O₃-SiO₂ nanocomposites. (2) Colloidal stability characteristics: Adding HCl is used to regulate the pH value of the solution, prevent the aggregation and precipitation of sol particles, and thus stabilize the sol system. (3) Ion exchange characteristics: By continuously adding deionized water and repeating ultrafiltration, solutes such as H⁺, Cl⁻, Fe³⁺,

Na⁺, and K⁺ in the sol can be washed away, thereby reducing the impact of these ions on the colloidal properties.

2.2 Research on the conductive properties of Al₂O₃-SiO₂ nanocomposite colloidal particles

Acidic polyaluminium chloride contains hydroxyl aluminum, while acidic silica sol contains hydroxyl silicon. Under certain conditions, dehydration condensation reaction can occur between aluminum hydroxyl and silicon hydroxyl [15]. The specific process is shown in Figure 2.

The original silica sol in Figure 2 is a stable system, but when the polyaluminum chloride sol is dripped, the original system balance will be destroyed [16,17]. Therefore, polyaluminum chloride was added dropwise, and dilute HCL was added during the process to maintain system stability [18]. The ratio of dripping polyaluminum chloride to silica sol is set to 1:1, 1:1.5, 1:2, 1:2.5, 1:3, 1:3.5, 1:4, 1:4.5, and 1:5. After the dropwise addition is completed, wait for 30 min to observe the sedimentation results. To verify the chargeability of Al₂O₃-SiO₂ nanocomposite colloid, the WY-2D/WY-3D electrophoresis measuring device (Fuzhou Jinshisu Instrument Equipment Co., Ltd) was used to measure the chargeability and electron migration rate of Al₂O₃-SiO₂ nanocomposite colloid particles. Before using the electrophoresis measurement device, first deeply clean the U-shaped tube, then inject the Al₂O₃-SiO₂ nanocomposite colloid until the colloid exceeds the valve openings at both ends of the U-shaped tube, then close the valve and inject Na₂CO₃ solution at both ends of the tube, and then the positive and negative poles of the power supply are connected to both ends of the U-shaped tube, and the power supply voltage is set to 220 V [19]. It was observed that the solution concentration at the negative end of the U-shaped tube increased significantly, while there was almost no silica sol at the positive end, indicating that the Al₂O₃-SiO₂ nanocomposite colloidal particles were positively charged.

2.3 Performance experiment of Al₂O₃-SiO₂ nanocomposite colloid repair building materials

2.3.1 Experiment on improving concrete porosity using Al₂O₃-SiO₂ nanocomposite colloidal particles

Choose $5 \times 5 \times 4$ cm concrete from the building materials (mixed with PC52.5 cement from Nanjing Red Lion Cement

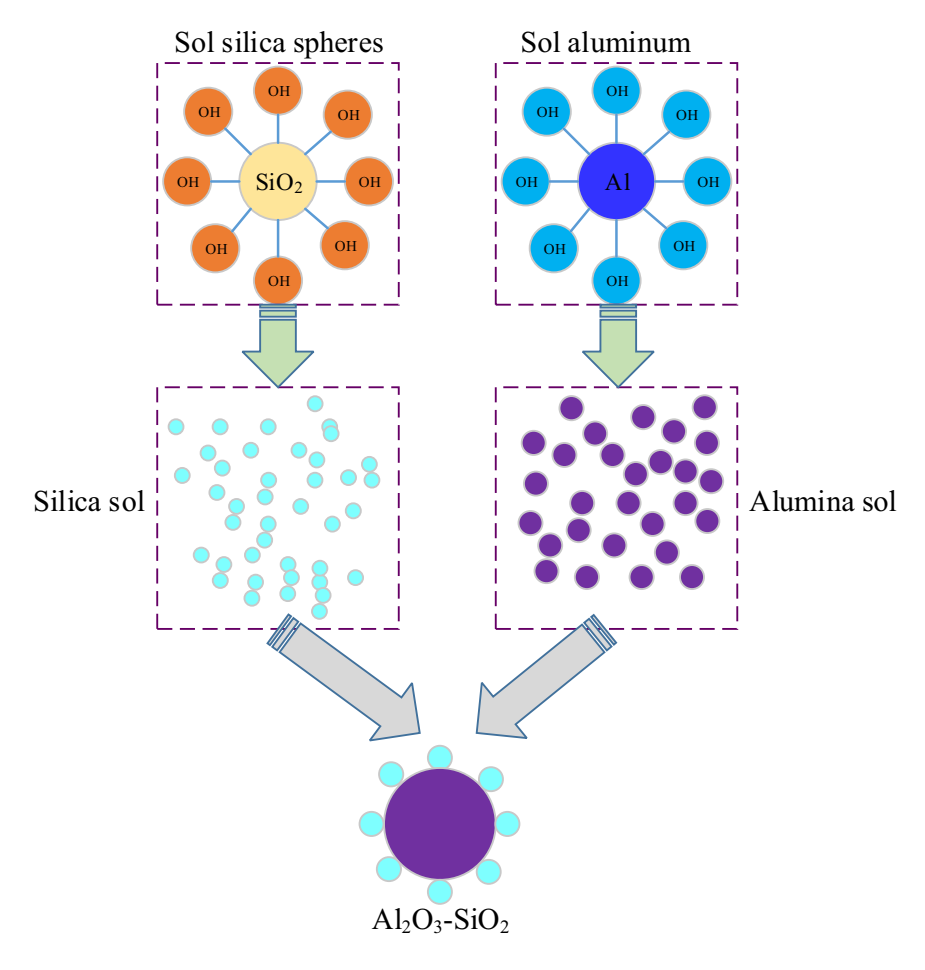


Figure 2: Al₂O₃-SiO₂ nanocomposite colloidal particle fusion model diagram.

Co., Ltd, I Class F fly ash from Nanjing Power Plant, and water-reducing agent from Shandong Mingjiang Chemical Co., Ltd) as the test object, and a self-made introduction device was used to introduce the Al_2O_3 – SiO_2 nanocomposite colloid into the concrete. The structural model of the introduction device is shown in Figure 3.

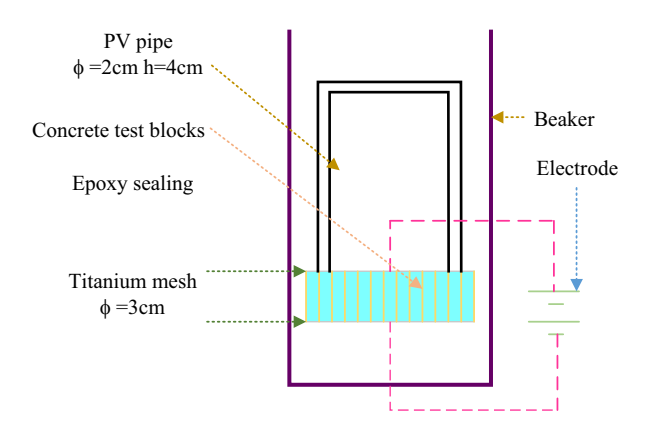


Figure 3: Schematic diagram of the structure of the device for introducing colloid into concrete.

According to the experimental steps shown in Figure 3, the PV pipe (Jiangsu Zhinai Pipe Industry Co., Ltd) was first sealed on the concrete sample using E-30CL glass glue (Wuxi Yongning Technology Co., Ltd). To make the concrete surface conductive, titanium mesh provided by Anping County Kunshi Wire Mesh Products Co., Ltd was used to wrap the upper and lower surfaces of the concrete samples. Next we connect the positive electrode of the power supply to the titanium mesh on the upper surface of the concrete, and the negative electrode to the titanium mesh on the lower surface of the concrete. After turning on the power, set the current to 15 mA and keep it powered on for a week. To accelerate the mobility of colloidal particles, 0.1 mol/L sodium hydroxide solution was added to the beaker to maintain the pH value of the concrete. Thereafter, the Al₂O₃–SiO₂ nanocomposite colloid needs to be replaced every day to ensure the stability of the experiment. On each day of the experimental process, when the colloidal particle introduction experiment was completed, concrete samples were taken out and labeled as sample 1, sample 2, sample 3, sample 4, and sample 5. Next the other five untreated surfaces of this sample were sealed using epoxy resin and curing agent [20]. In addition, for comparative experiments, untreated concrete samples under the same conditions were selected, labeled as sample 6, sample 7, sample 8, sample 9, and sample 10, respectively. Before conducting water absorption and dehydration experiments, each sample was weighed and soaked in pure water for 5 h. Afterwards, the sample was removed and weighed again. Subsequently, the samples were placed in a drying oven for drying and were taken out every 2 h and weighed again. By measuring the water absorption and dehydration of each sample, the purpose is to study the application of $Al_2O_3-SiO_2$ nanocomposite colloid in concrete to evaluate its improvement effect on concrete porosity [21,22].

Next the solution in the beaker in the device in Figure 3 was replaced differently, and the experiment was conducted according to the same operating steps. First, replace the solutions in the beaker with 0.1 mol/L sodium hydroxide solution, 9% sodium chloride solution, and plasma water. The concrete samples were then removed and placed into specimen bags after drying. To obtain roughly the same sample fragments, crush the samples with a hammer, take out the fragments from each sample, and label them as sample a (0.1 mol/L sodium hydroxide solution) and sample b (9% sodium chloride solution), and sample c (plasma water). The untreated sample is labeled sample d. For the examination of the individual samples, a D8 ADVANCE X-ray diffractometer (produced by the manufacturer BRUKER) was used. During the detection process, the tube voltage of the diffractometer was set to 50 kV, the tube current was 35 mV, the scanning speed was 20°/min, and the scanning angle range was from 0° to 90°. In addition, fragments of approximately $3 \times 3 \times 3$ cm were selected from the crushed samples, and mercury intrusion experiments were conducted on the fragmented samples using the AutoPore IV JK-YG2000 Jingkorida fully automatic mercury intrusion instrument.

2.3.2 Research on the anti-corrosion effect of Al₂O₃-SiO₂ nanocomposite colloidal particles on steel bars

Q345 hot-rolled steel sheets were selected as a substitute for concrete steel bars to study the anti-corrosion effect of Al_2O_3 – SiO_2 nanocomposite colloidal particles on steel bars. Cut the Q345 hot-rolled steel sheet into a 20 × 20 × 2 cm sample, and then polish the steel sheet sample smoothly with 400 mesh, 800 mesh, 1,200 mesh, and 1,600 mesh sandpaper, then further polish it on a polishing machine, and then clean it with alcohol. The steel sheet was finally rinsed with deionized water [23,24]. In the experiment, a

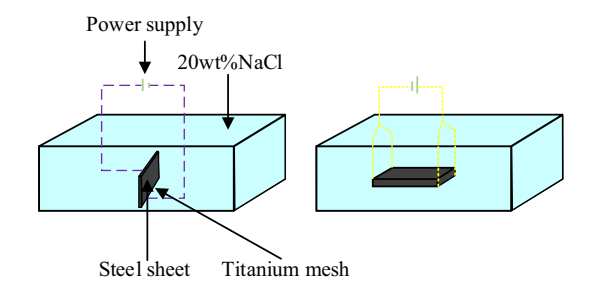


Figure 4: Schematic diagram of the self-made steel corrosion simulation device.

self-made steel corrosion simulation device was used to conduct the test. The schematic diagram of the device structure is shown in Figure 4. Through this device, we can simulate the corrosion of steel bars in a real environment and evaluate the protective effect of Al_2O_3 – SiO_2 nanocomposite colloidal particles on steel bars.

According to the experimental device shown in Figure 4, the sample steel piece is wrapped in a titanium mesh, and one end is connected to the negative electrode of the power supply through a wire, and the other end is connected to the positive electrode of the power supply. Use 20 wt% NaCl solution as the corrosive liquid, and the corrosion current provided by the power supply is 15 mA. To simulate corrosion of steel bars, two sets of experiments were conducted, labeled Group 1 and Group 2, respectively. In Group 1, the steel sheet samples were protected by Al₂O₃-SiO₂ nanocomposite colloidal particles, while in Group 2, the steel sheet samples were not protected by Al₂O₃-SiO₂ nanocomposite colloidal particles. The samples in both groups of experiments were energized and corroded for 12 h. The corrosion resistance and corrosion Tafel curve tests were conducted on two sets of steel sheet samples using a DH7000 series electrochemical workstation [25-27].

3 Result analysis

3.1 Settlement experiment results

The results of the Al_2O_3 – SiO_2 nanocomposite colloid sedimentation experiment obtained using nine mixing ratios are shown in Figure 5.

It can be seen from Figure 5 that when the mass ratio of silica sol to polyaluminum chloride is 1:2.5, the deposition height of the liquid in the test tube is relatively low. At this time, the degree of colloid aggregation is not high, the

6 — Dingyu Ni et al. DE GRUYTER

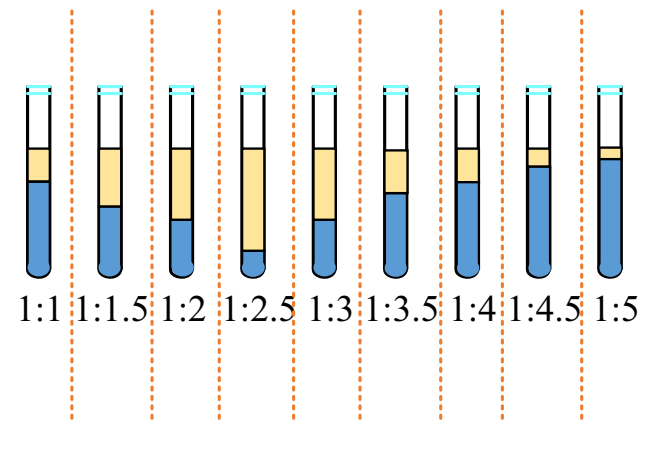


Figure 5: Comparison of sedimentation results of Al_2O_3 - SiO_2 nanocomposite colloids with different ratios.

dispersion is good, and it is easy to penetrate into the building materials and improve the building material performance. Therefore, the ${\rm Al_2O_3-SiO_2}$ nanocomposite colloid prepared in subsequent experiments will be based on this ratio. In order to further observe the dispersion of colloidal particles, an LVEM5 desktop transmission electron microscope was used to observe the morphological characteristics of three types of particles: silica sol, polyaluminum chloride, and ${\rm Al_2O_3-SiO_2}$ nanocomposite colloid. The results are shown in Figure 6.

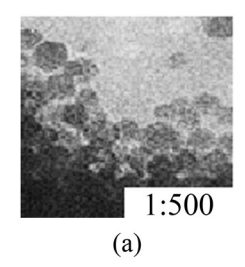
Figure 6 shows the morphological structures of three different types of nanoparticle sols. In Figure 6(a), the shape of the silica sol colloidal particles is spherically distributed, and the average particle size distribution is between 10.5 and 17.5 nm. Although there is a slight agglomeration of colloidal particles locally, the overall distribution of colloidal particles is relatively uniform and uniform. The distance between colloidal particles is small. Correspondingly, in Figure 6(b), the morphology of the polyaluminum chloride sol exhibits a two-dimensional chain distribution with a chain width size of 1–5 nm. These chain-shaped polyaluminum chloride sol is compounded to the surface of the silica sol colloidal particles in the state of chain belts to form a coating structure. In Figure 6(c), the Al₂O₃–SiO₂

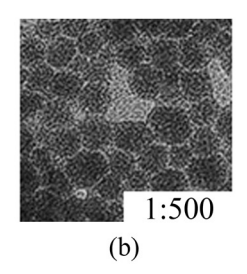
nanocomposite colloidal particles present a core-shell coating structure. Among them, the core layer is silica sol colloidal particles with a size of 10.5–17.5 nm. The shell layer is formed by polyaluminum chloride sol chain belts, and its size is about 2 nm. In general, the morphological structures of the three types of nanoparticle sol all show a relatively obvious coating type, and the colloidal particles are evenly dispersed without obvious agglomeration.

3.2 Porosity experimental test results

In the porosity experiment, the absorption-dehydration test results of ten groups of concrete samples are shown in Figure 7.

Figure 7(a) is the experimental group, showing the water absorption-dehydration test results of concrete samples treated with Al₂O₃-SiO₂ nanocomposite colloid. During the water absorption stage (0-5 h), we observed that samples 1–5 absorbed approximately 0.563, 0.756, 1.123, 0.486, and 1.065 g of water, respectively. During the gradual dehydration stage from 5-15 h, we observed that samples 1-5 dehydrated 0.732, 1.956, 0.568, 1.452, and 2.358 g of water, respectively. On the other hand, Figure 7(b) is the control group, showing the water absorption-dehydration test results of untreated concrete samples. During the water absorption stage, we observed that samples 6–10 absorbed approximately 4.358, 3.245, 3.248, 2.635, and 3.745 g of water, respectively. During the dehydration stage, we observed that samples 6-10 dehydrated 7.358, 5.142, 4.856, 4.365, and 4.215 g of water, respectively. By comparing these two sets of data, we can find that during the water absorption stage, the water absorption of untreated concrete samples is significantly higher than that of concrete samples treated with Al₂O₃-SiO₂ nanocomposite colloid, which indicates that untreated concrete samples have higher porosity. At the same time, this also shows that Al₂O₃-SiO₂ nanocomposite colloid can improve the porosity of concrete to a certain extent. During the





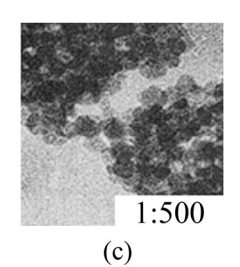


Figure 6: TEM patterns of (a) silica sol, (b) polyaluminum chloride, and (c) Al₂O₃-SiO₂.

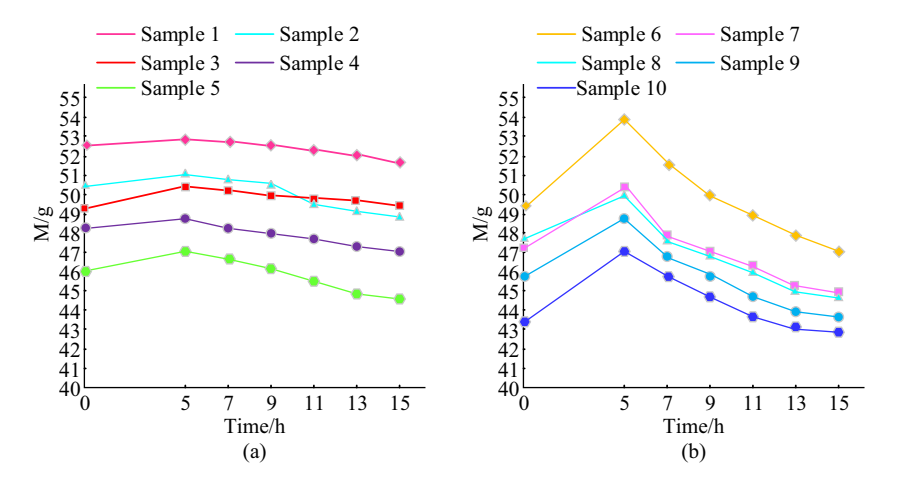


Figure 7: Absorption-dehydration test results of concrete samples. (a) Experimental group and (b) control group.

dehydration stage, the slopes of the curves of the untreated concrete samples are all larger, while the curves of the treated concrete samples are relatively gentle. This shows that the untreated concrete loses water at a faster rate, and further indicates that the Al_2O_3 – SiO_2 nanocomposite colloid can reduce the void ratio, improve the performance of concrete, and prevent the erosion of harmful foreign particles. The results of using an X-ray diffractometer to detect the XRD patterns of samples a–d are shown in Figure 8.

In Figure 8, it can be seen that different concrete samples were treated differently, and their crystal structure and content were determined through testing and analysis. Sample d was not subjected to any treatment, and the test results showed that the main crystal forms in the sample were $\text{Ca}(\text{OH})_2$ and $\text{CaAlSiO}_4(\text{OH})_8$. Sample a was treated with sodium hydroxide, and the test results showed that the peaks of $\text{CaAlSiO}_4(\text{OH})_8$ and $\text{Ca}(\text{OH})_2$ crystal forms in this sample were more pronounced than those in sample d. This is because the $\text{Al}_2\text{O}_3\text{-SiO}_2$ nanocomposite colloidal

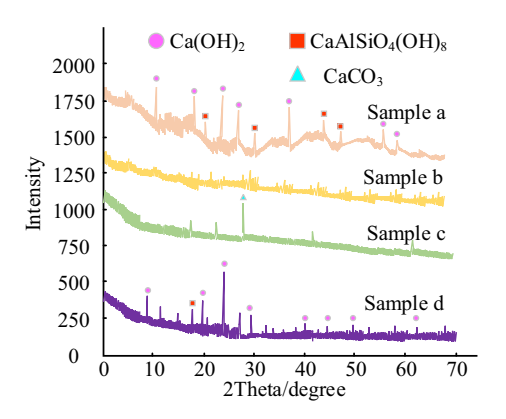


Figure 8: XRD patterns of four samples.

particles in the concrete react with sodium hydroxide to generate $CaAlSiO_4(OH)_8$, making the $CaAlSiO_4(OH)_8$ in sample a more pronounced. Samples b and c were treated with sodium chloride and ionic water, respectively. The test results showed that the peak intensities of $CaAI-SiO_4(OH)_8$ and $Ca(OH)_2$ crystal forms in these two samples were relatively weak, indicating that their content was relatively low. This is because there is a layer of $Al_2O_3-SiO_2$ nanocomposite colloidal sol on the surface of the sample, and these sols are amorphous substances. Therefore, the peaks of $CaAISiO_4(OH)_8$ and $Ca(OH)_2$ are very few in these two samples.

The test results of the mercury injection experiment using fully automatic mercury injection on samples a–c are shown in Figure 9.

According to the test results of the cumulative mercury injection amount of the sample shown in Figure 9(a), it can be seen that the cumulative mercury injection amount of sample a treated with sodium hydroxide, sample b treated with sodium chloride, and sample c treated with ionized water are 0.945, 0.964, and 0.927 mL/g, respectively. These values represent the volume of liquid mercury entering the pores of the sample. Judging from the test results, there is little difference in the porosity of the samples obtained from the three different processing media. This indicates that no matter which medium is used to treat the sample, it does not significantly affect the porosity of the sample. At the same time, the pore size distribution of the sample is shown in Figure 9(b). This figure shows that the pore size distribution of the sample is relatively dense in the range of 100-1,000 nm. This shows that the sample gaps within this range are filled by Al₂O₃-SiO₂ nanocomposite colloidal particles, and the filling effect is good. And the control range of colloidal particles is 50-300 nm, which further illustrates that Al₂O₃-SiO₂ nanocomposite colloidal particles

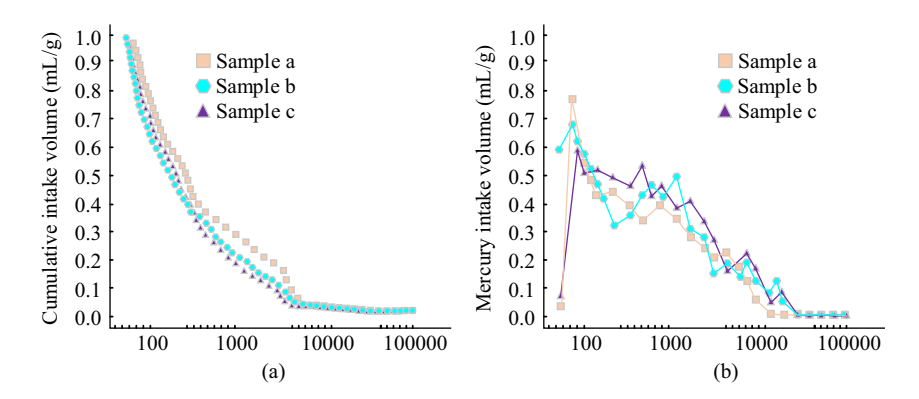


Figure 9: Test results of mercury injection experiment. (a) Accumulated mercury intrusion into the sample and (b) the pore size distribution of the sample.

can effectively fill concrete samples and prevent the erosion of harmful external solutions.

3.3 Steel corrosion simulation test results

The AC impedance test range of the DH7000 electrochemical workstation was set to 50 μ Hz to 7 Hz, and the scanning speed was 0.002 V/s. The test results of the sample corrosion impedance were fitted on the impedance spectrum fitting software Zview. The results are shown in Figure 10.

It can be seen from Figure 10 that as the corrosion time increases, the radius of curvature of the curve of the steel sheet sample increases. The larger the radius of curvature, the greater the reaction resistance, the more difficult it is for the electrochemical reaction on the surface of the steel sheet to proceed, and the slower the corrosion rate. Comparing Figure 8(a) and (b), the curvature radius of steel

sheet samples protected by Al₂O₃-SiO₂ nanocomposite colloidal particles is generally larger than that of steel sheet samples without protection. It shows that Al₂O₃-SiO₂ nanocomposite colloidal particles can effectively prevent the electrochemical reaction on the surface of the steel sheet and prevent the steel sheet from being corroded. In order to further characterize the corrosion resistance of the sample, the AC impedance value of the sample was tested using an equivalent circuit. When the steel sheet sample of Group 1 was corroded for 0, 4, 8, and 12 h, its AC impedance value was 120.1, 263.8, 345.6, and 421.9, respectively. When the steel sheet samples of Group 2 were corroded for 0, 4, 8, and 12 h, their AC impedance values were 120.1, 386.3, 456.8, and 589.6, respectively. The AC impedance value of the steel sheet sample protected by Al₂O₃-SiO₂ nanocomposite colloid is significantly smaller than that of the unprotected steel sheet sample, indicating that the Al₂O₃-SiO₂ nanocomposite colloid promotes the corrosion protection performance of steel bars. In addition, the corrosion Tafel curve

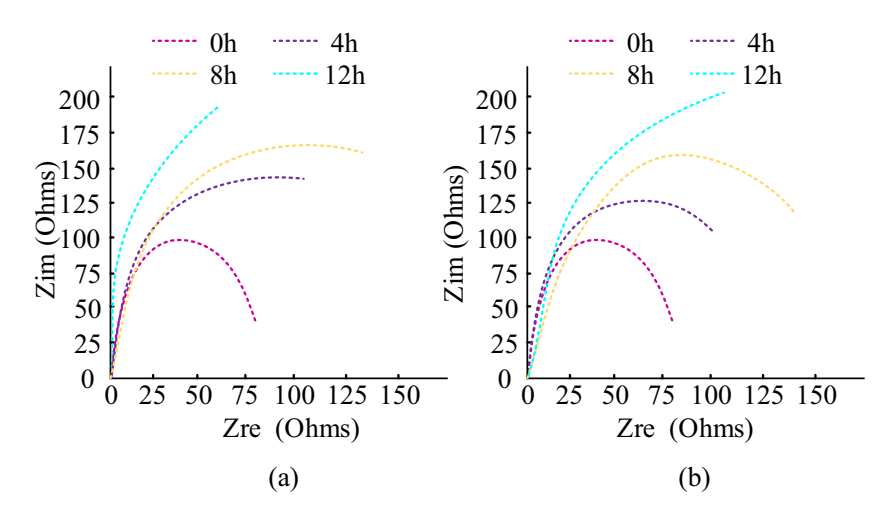


Figure 10: Test results of corrosion resistance of two groups of samples. (a) Group 1 and (b) Group 2.

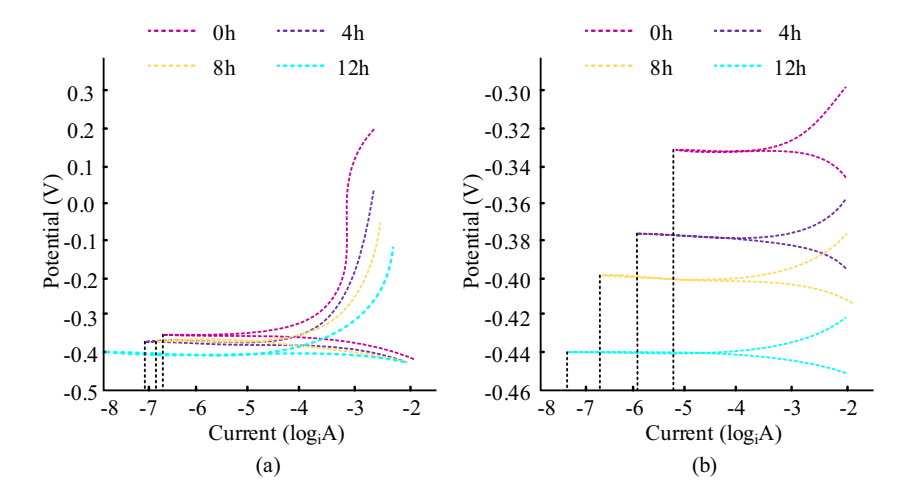


Figure 11: Corrosion Tafel curve of sample. (a) Group 1 and (b) Group 2.

of the sample was also tested, and the results are shown in Figure 11.

It can be seen from Figure 11(a) that when the steel sheet sample of Group 1 is corroded for 0, 4, 8, and 12 h, the logarithm of the corrosion current is approximately -6.7, -6.8, -7.1, and -8.0, respectively. It can be seen from Figure 11(b) that when the steel sheet sample of Group 2 is corroded for 0, 4, 8, and 12 h, the logarithm of the corrosion current is approximately -5.2, -5.9, -6.8, and -7.3, respectively. It shows that for the same corrosion time, the corrosion current logarithm values of steel sheet samples protected by Al_2O_3 – SiO_2 nanocomposite colloid are lower than those of unprotected steel sheet samples. And as the

corrosion time progresses, the logarithmic value of the corrosion current of the steel sheet sample gradually becomes smaller. This also shows that the $\rm Al_2O_3-SiO_2$ nanocomposite colloid promotes the corrosion protection performance of steel bars. To more specifically observe the morphology of the steel sheet samples with and without protection, the steel sheet samples of Groups 1 and 2 were observed using a 1,000× scanning electron microscope. The results are shown in Figure 12.

Figure 12(a) shows a steel sheet sample protected by Al_2O_3 – SiO_2 nanocomposite colloid. It can be seen that as the corrosion time progresses, the metallic luster of the steel sheet sample darkens slightly, but there are no corrosion

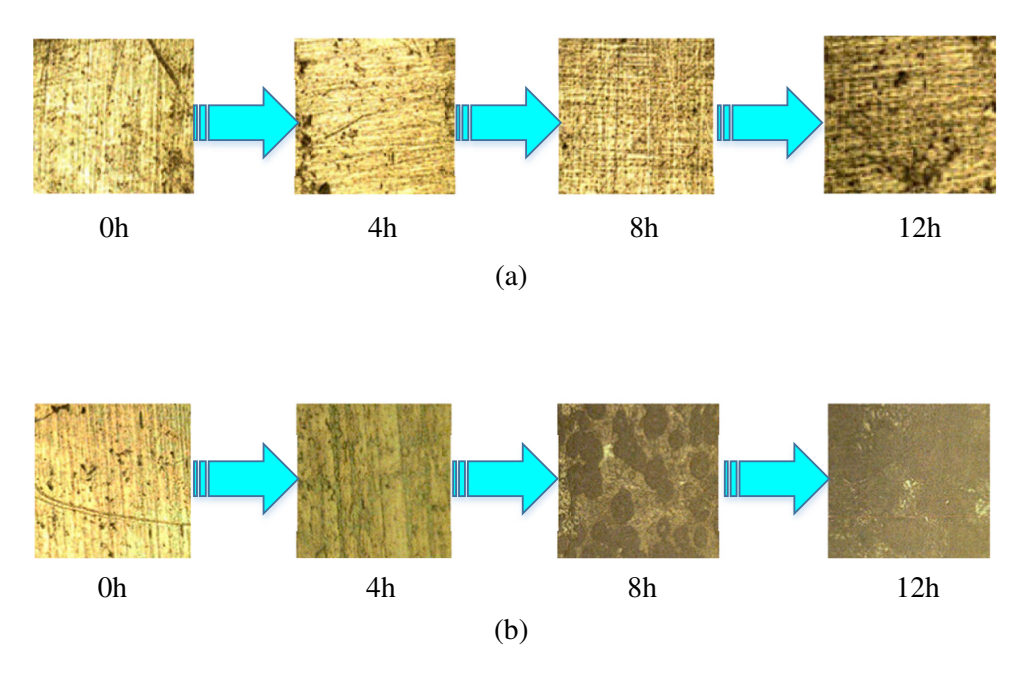


Figure 12: Comparison of morphology observation results of steel sheet samples. (a) Group 1 and (b) Group 2.

spots and the degree of corrosion is very small. Figure 12(b) shows the unprotected steel sheet sample. It can be seen that as the corrosion time progresses, the metal of the steel sheet sample becomes darker and darker, and corrosion spots appear after 4 h of corrosion. Subsequently, the corrosion spots became larger and larger, and the degree of corrosion also increased. It shows that the Al_2O_3 – SiO_2 nanocomposite colloid can effectively protect the steel sheet sample and prevent the steel sheet from being corroded.

4 Discussion

To quickly repair and protect building materials such as reinforced concrete, Al₂O₃-SiO₂ nanocomposite colloid was prepared using silica sol and polyaluminum chloride. The basic properties of the colloidal particles were first tested, and the results showed that the colloidal particles were positively charged, the size of the colloidal particles was 12.5-19.5 nm, the degree of aggregation was not high, and the dispersion was good. These properties are conducive to penetrating into building materials and improving the performance of building materials. The colloidal particles were applied to the concrete surface, and it was found that the water absorption of the concrete samples treated with Al₂O₃-SiO₂ nanocomposite colloidal particles was significantly reduced and the dehydration rate was slower. Moreover, the pore size distribution of concrete repaired by colloidal particles is relatively dense in the range of 100–1,000 nm, while the control range of colloidal particles is 50-300 nm. It shows that Al₂O₃-SiO₂ nanocomposite colloidal particles can reduce the void ratio, improve the performance of concrete, and prevent the erosion of harmful foreign particles. The colloidal particles were applied to the surface of steel bars and it was found that the AC impedance value of the steel sheet sample protected by the Al₂O₃–SiO₂ nanocomposite colloid was significantly smaller than that of the unprotected steel sheet sample, and the corrosion current of the steel sheet sample protected by the Al₂O₃-SiO₂ nanocomposite colloid had numerical values lower than those of the unprotected steel sheet samples. This shows that the colloid plays a positive role in promoting the corrosion protection performance of steel bars. In the morphology observation of the steel sheet, it was found that as the corrosion time progressed, the metallic luster of the steel sheet sample protected by the Al₂O₃-SiO₂ nanocomposite colloid darkened slightly, but there were no corrosion spots and the degree of corrosion was very small. This shows that the colloid can effectively protect steel bars from corrosion. Although the colloidal particles have a significant

protective effect on concrete and steel reinforcement, there are also some issues. First, its construction process requires special equipment and technology, which poses certain difficulties for specific regions. Second, it is uncertain whether the colloidal particles have long-term protective effects and durability. In addition, different building materials and environmental conditions may require different ratios of Al_2O_3 – SiO_2 nanocomposite colloids for repair and protection. Subsequent experiments will be conducted to address these issues one by one.

Funding information: The Science and Technology Project of Wenzhou Science & Technology Bureau (Grant No. ZS2022002), the Science and Technology Project of Wenzhou Science & Technology Bureau (Grant No. S20220029), Zhejiang Provincial Department of Education research project (Y202353099) and Zhejiang NAVEC Scientific & Research Project (Grant No. ZJCV2023B34).

Author contributions: Dingyu Ni: conceptualization, formal analysis, investigation, data curation, and writing – original draft preparation; Shengliang Lu: conceptualization, methodology, validation, writing – original draft preparation, writing – review and editing, and project administration; Feng Cai: formal analysis, investigation, and visualization.

Conflict of interest: There is no conflict of interests in this manuscript.

Data availability statement: The datasets generated during and/or analyzed during the current study are available from the corresponding author on reasonable request.

Ethical approval: Ethical approval: The conducted research is not related to either human or animal use.

References

- [1] Sococol I, Mihai P, Toma IO, Olteanu-Donţov I, Venghia V-M. Stress-Strain relation laws for concrete and steel reinforcement used in non-linear static analytical studies of the moment resisting reinforced Concrete (RC) frame models. Bull Polytech Inst Iaşi. 2021;67(1):17–29.
- [2] Lsmael AO, Ghareb AHYS. Effect bonding strength steel reinforcement with epoxy coating on the character destruction of autoclaved aerated concrete beams in bending. Mater Sci Forum. 2020;74(974):665–71.
- [3] Berrocal CG, Fernandez I, Bado MF, Casas JR, Rempling R. Assessment and visualization of performance indicators of reinforced concrete beams by distributed optical fibre sensing. Struct Health Monit. 2021;20(6):3309–26.

- [4] Liu Y, Hao H, Hao Y, Cui J. Experimental study of dynamic bond behaviour between corroded steel reinforcement and concrete. Constr Build Mater. 2022;356(21):658-71.
- [5] Dong G, Wu J, Zhao X. Fatigue performance of recycled aggregate concrete beams with corroded steel reinforcement. ACI Struct J. 2022;119(2):123-37.
- Aykac B, Yavuzcan A. Repair of damaged reinforced concrete beams by epoxy injection. Rev Rom Mater. 2022;52(4):394-403.
- Bahij S, Omary S, Feugeas F, Faqiri A. Structural strengthening/ repair of reinforced concrete (RC) beams by different fiber-reinforced cementitious materials - a state-of-the-art review. Eur J Environ Civ En. 2020;10(4):1-15.
- Wang Y, Liu Y, Feng W, Zeng S. Waste haven transfer and povertyenvironment trap: evidence from EU. Green Low-Carbon Econ. 2023;1(1):1-11.
- Liu K, Sun Y, Yang D. The administrative center or economic center: which dominates the regional green development pattern? A case study of Shandong peninsula urban agglomeration, China. Green Low-Carbon Econ. 2023;1(3):110-20.
- [10] Taheri S, Giri P, Ams M, Bevitt JJ, Bustamante H, Madadi M. Migration and formation of an iron rich layer during acidic corrosion of concrete with no steel reinforcement. Constr Build Mater. 2021;309(22):125105.1-14.
- [11] Nojehdehian H, Mashhadi HA, Rahimi HR, Salehi A. Y-TZP/nAl₂O₃/ nSiO₂ nanocomposites for restorative dentistry applications. Int J Mater Eng Technol. 2020;19(1):17-33.
- [12] Jabraeili M, Pourdarbani R, Najafi B, Salehi A. Modelling the effects of Al₂O₃-SiO₂ nanocomposite additive in biodiesel-diesel fuel on diesel engine performance using hybrid ANN-ABC. Acta Technol Agric. 2021;24(1):20-6.
- [13] Yu Z, Yang D, Wang R, Jiang Q, Zhu K, Cui J. Investigation on properties of Al₂O₃-SiO₂ complex shaped refractory fabricated by layered extrusion forming. Ceram Int. 2020;46(11):18985-93.
- [14] Xu C, Wang C, Xu R, Zhang J, Jiao KX. Effect of Al₂O₃ on the viscosity of CaO-SiO₂-Al₂O₃-MgO-Cr₂O₃ slags. Int J Min Met Mater. 2021;28(5):797-803.
- [15] Yu LC, Lai YL, Lin MW, Shiu HW, Lin JH, Wei DH. Modulating the magnetic coupling in paramagnetic Co nanoparticles embedded in tris(8-hydroxyquinoline) aluminum for spintronics applications. ACS Appl Nano Mater. 2021;4(5):5240-9.

- [16] Peng L, Jiang W, Yang L, Chen Z, Li G, Guan F. Effect of silica sol on performance and surface precision of alumina ceramic shell prepared by binder jetting. Ceram Int. 2022;48(17):24372-82.
- Pan D, Liu C, Yi J, Li X, Li F. Different effects of foliar application of [17] silica sol on arsenic translocation in rice under low and high arsenite stress. J Environ Sci. 2021;105:22-32.
- Song W, Zeng J, Li X, Xie Y, Wu X. Cyanobacterial biomass: a striking factor to decrease polyaluminium chloride (PACI) coagulation efficiency during a successive bloom. Water Sci Tech Sup. 2021;21(7):4195-204.
- [19] Huang G, Xu B, Qiu J, Peng L, Han P. Symmetric electrophoretic light scattering for determination of the zeta potential of colloidal systems. Colloid Surf A. 2020;587(4):124339.1-6.
- Odevemi SO, Abdulwahab R, Bello SA, Omonivi AO, Adenivi G. Repair of flexural damaged reinforced concrete beams using embedded bamboo reinforced epoxy composite. Malaysian J Civ Eng. 2020;32(1):13-8.
- [21] Pan X, Yang TY. Postdisaster image-based damage detection and repair cost estimation of reinforced concrete buildings using dual convolutional neural networks. Comput-Aided Civ Infrastruct. 2020:35(5):495-510.
- [22] Akkaya A, Aatay SH. Investigation of the density, porosity, and permeability properties of pervious concrete with different methods. Constr Build Mater. 2021;294:123539.
- [23] Tiwari A, Xu F, Lakhtakia A, Yamaguchi H, Bukkapatnam STS. On colors of stainless-steel surfaces polished with magnetic abrasives. Appl Opt. 2021;60(9):2549-59.
- Frazee GR. Allowable external loading of buried smooth-wall steel [24] piping: parametric evaluation using the latest guidance. J Pipeline Syst Eng. 2022;13(1):4021081.1-9.
- [25] Liu D, Xie X, Roscher J, Holze R. Comparative study of the corrosion stability of dental amalgams with electrochemical impedance measurements. Mater Corros. 2020;71(6):949-55.
- [26] Darmawan A, Rasyid SA, Astuti Y. Modification of the glass surface with hydrophobic silica thin layers using tetraethylorthosilicate (TEOS) and trimethylchlorosilane (TMCS) precursors. Surf Interface Anal. 2021;53(3):305-13.
- Darmawan A, Saputra RE, Astuti Y. Structural, thermal and surface properties of sticky hydrophobic silica films: effect of hydrophilic and hydrophobic precursor compositions. Chem Phys Lett. 2020:761:138076.